PAPER

Dual measurement self-sensing technique of NiTi actuators for use in robust control

IOP Publishing Smart Materials and Structures
Smart Mater. Struct. **26** (2017) 105050 (10pp) https://doi.org/10.1088/1361-665X/aa8b42

Dual measurement self-sensing technique of NiTi actuators for use in robust control

Austin Gurley[1], **Tyler Ross Lambert**, **David Beale and Royall Broughton**

1418 Wiggins Hall, 354 War Eagle Way, Auburn University, AL, 36849, United States of America

E-mail: arg0007@tigermail.auburn.edu, trl0007@tigermail.auburn.edu, bealedg@auburn.edu and brougrm@auburn.edu

Received 9 June 2017, revised 8 September 2017
Accepted for publication 8 September 2017
Published 22 September 2017

Abstract

Using a shape memory alloy actuator as both an actuator and a sensor provides huge benefits in cost reduction and miniaturization of robotic devices. Despite much effort, reliable and robust self-sensing (using the actuator as a position sensor) had not been achieved for general temperature, loading, hysteresis path, and fatigue conditions. Prior research has sought to model the intricacies of the electrical resistivity changes within the NiTi material. However, for the models to be solvable, nearly every previous technique only models the actuator within very specific boundary conditions. Here, we measure both the voltage across the entire NiTi wire and of a fixed-length segment of it; these dual measurements allow direct calculation of the actuator length without a material model. We review previous self-sensing literature, illustrate the mechanism design that makes the new technique possible, and use the dual measurement technique to determine the length of a single straight wire actuator under controlled conditions. This robust measurement can be used for feedback control in unknown ambient and loading conditions.

Keywords: shape memory, control, robotics, smart materials

(Some figures may appear in colour only in the online journal)

Nomenclature

ρ	Electrical resistivity
T	Temperature
ξ	Martensite phase fraction
σ	Stress
R	Electrical resistance
A	Cross-sectional area
ϵ	Strain
r_0	Initial wire radius
ℓ_0	Initial wire length
L	Wire length
V	Voltage
I	Electrical current
A_f	'Austenite finish' temperature, at which SMA material is fully contracted

[1] Author to whom any correspondence should be addressed.

1. Introduction

A clear obstacle to creating robot dexterity is in limits to their versatile poses—the degrees of freedom (DoF) in their motion. While computer science is quickly finding ways to control high DoF robots (deep learning, for instance) [1], the hardware is not keeping pace. For example, computer graphics in film can reconstruct 244 DoF in the human body and convince millions of movie-goers that they have seen a living being [2]. The most pressing obstacle to dexterity and dexterous manipulation in modern robotics applications is physical DoF [3].

Today, actuator design is the limiting factor—motors, pneumatics, and hydraulics are simply too heavy and too big

to package hundreds of DoF in a single system. This is particularly apparent at small scales—common ants have over 20 useful DoF that have been mimicked in prior research [4], but there is no mechanical motor today that can match an ant's leg in size and strength. For commercial applications of highly dexterous robotics to become viable, the actuators that give the robots their dexterity must be extremely low cost because many more actuators will be needed than in more traditional systems. The ideal actuator must provide extremely high strength-per-weight, while allowing many to fit in a small space $\left(\frac{\text{DoF}}{\text{m}^2}\right)$, at low cost $\left(\frac{\$}{\text{DoF}}\right)$. This research outlines how shape memory alloys (SMA) can be utilized to create actuators that fit this mold. A primary discovery of this work is a self-sensing technique that allows accurate control of simple SMA wire actuators.

Because both the models and controls are very complex, SMA actuators have not become prevalent in robot or machine design except in places where binary (two-position) motion is all that is needed. Binary control allows the model to be as simple as two known positions; the state of the SMA when heated and when cold. A more useful actuator will be easily commanded to obtain a desired position (or force) anywhere within its range of capability, not just at the limits. In order to accomplish this, a position (force) sensor is generally used in a feedback loop with the actuator. While sensor feedback is feasible in many cases, the great benefits of SMA actuators (high payload-to-weight ratios, simplicity, and small size) cannot usually be realized in this configuration because the added sensor adds complexity, weight and volume. Ideally the changing electrical properties of the SMA material itself could be used as a position (load) sensor. Because the behavior of the SMA motion and electrical properties are nonlinear and exhibit hysteresis, it has proven difficult to create a robust self-sensing control scheme [5–7]. No previous research has successfully modeled the electrical properties accurately for general loading and ambient conditions —this is crucial for a robotic actuator since the 'artificial muscle' must control motion under varying loads and reject disturbances during use.

We have developed an SMA actuator 'dual measurement' method that allows self-sensing without complex models. This method is simple, only requiring one additional voltage measurement at a stationary point along the length of the actuator, and can easily be incorporated in practical robotic devices. By making the secondary measurement, the length of the actuator can be calculated directly and accurately with no assumptions about ambient conditions or loads except that they are constant along the entire actuator length. The method is not affected by hysteresis, twinning, or *R*-phase transformations which cause other methods to fail.

In this work, we begin by reviewing existing SMA self-sensing techniques, in particular resistivity modeling and attempts to utilize measurements of wire resistance to determine actuator length. While these models do seem to capture the material behavior correctly, this work finds that no previous self-sensing method is robust to both unknown ambient conditions and unknown loads. Our robust dual measurement technique is described, and relevant equations are derived. An experiment is performed that shows the robust length sensing ability of the actuator. The dual measurement technique is compared to the use of resistance alone, and shown to be superior. A control example with several relevant scenarios demonstrates the ability of the dual-measurement condition to remain accurate in conditions that cause the resistance-based methods to fail. Finally, the accuracy improvements of this method, and potential sources of inaccuracy if the method is incorrectly applied, are discussed.

2. Background and literature review

2.1. Resistance modeling

It has been generally accepted in the SMA community for many years that the resistance of SMA materials can be used for self-sensing of strain. However, when trying to apply the concept, it is found that strain is only one component of the resistance variation; the actual response is affected by strain, stress, temperature, and martensite phase fraction. In many cases, the easy solution is to assume the wire position is proportional to heating power applied [6], or to operate the actuator in only two positions at the end of the travel [8, 9]. Because of the large effect of transformation on strain (compared to other terms in the constitutive model) it has been proposed in several works that the relationship between strain and resistance is sufficiently linear to use for control [10, 11]. Wu has shown that the resistance is a very linear function of strain for super-elastic wires at constant temperature [12].

However, a more general sensing technique should allow control to intermediate positions. Most researchers approach self-sensing by modeling the resistivity of the material and the change with temperature, load and crystal phase fraction. A model employed by several researchers is the linear phase-fraction model with temperature dependent coefficients. Ikuta (1991) modeled the electrical resistivity (ρ) of an SMA wire as a function of martensite phase fraction (ξ) consistent with the 'Voigt model' of the SMA [13, 14]:

$$\rho = (1 - \xi)\rho_{\text{A}} + \xi\rho_{\text{M}}. \tag{1}$$

ρ_{A} and ρ_{M} denote resistivities of the material in austenite and martensite phases, respectively. The resistivity of each phase can be computed as a function of the wire temperature:

$$\rho_{\text{A}} = \rho_{\text{A0}} + \alpha_{\text{A}}(T - T_0), \tag{2}$$

$$\rho_{\text{M}} = \rho_{\text{M0}} + \alpha_{\text{M}}(T - T_0). \tag{3}$$

T is the temperature of the wire actuator, T_0 is the initial measured temperature of the wire, α_{M} and α_{A} are the temperature dependence of the resistivity, and ρ_{M0} and ρ_{A0} are known quantities of the resistivities at the initial measured temperature. This model is simplified by neglecting the additional terms that account for the *R*-phase; *R*-phase transformation confuses many experimental results as it seems to behave macroscopically like martensite, but has very different electrical resistivity than either martensite or

austenite [15]. It has been demonstrated in many cases that transformation to the *R*-phase can be precluded by maintaining actuator stress above a critical value, often given as approximately 150 MPa [10]. The *R*-phase can also be eliminated by shape-setting at high temperatures, though this may have other adverse effects [16]. To be certain the change in electrical resistivity is due to crystal transformation and not another mechanism, Antonucci confirmed the effect of the crystal phases on resistivity using differential scanning calorimetry [15].

However, attempts at self-sensing with varying temperatures and stresses further complicate the model. Novak uses a similar model to Ikuta and adds an additional correction term for the resistivity dependence on wire stress (β_A, β_M) [17]:

$$\rho_A = \rho_{A0} + \alpha_A(T - T_0) + \beta_A\sigma, \tag{4}$$

$$\rho_M = \rho_{M0} + \alpha_M(T - T_0) + \beta_M\sigma. \tag{5}$$

These equations again neglect the *R*-phase components of the model, since it can be eliminated by preloading. This does indeed fit better to experimental data than the Ikuta model, especially for constant stress [17–20].

There is, however, a realistic and more practical interpretation of the impact of applied stress than the addition of a stress term to the formulation of the resistivity. Because the stress causes strain (change in length) and contraction of area (due to Poisson contraction), the additional resistance can be found to be caused by this elastic strain and modeled by the definition of resistance [21–23]. This can be modeled by noting that the wire resistance is defined as linearly proportional to the resistivity:

$$R = \frac{\rho L}{A}. \tag{6}$$

R denotes the total resistance of the wire, L denotes the length of the SMA actuator and A denotes the cross-sectional area of the SMA wire. Both properties can be found in terms of initial wire dimensions and the wire stress and strain [24]:

$$L = \ell_0(1 + \epsilon), \tag{7}$$

$$A = \pi r_0^2\left(1 - \frac{\nu\sigma}{E}\right)^2. \tag{8}$$

ϵ denotes the elastic component of strain, r_0 the initial wire radius, ℓ_0 the initial wire length, E is the elastic modulus, and ν is the wire's Poisson ratio.

It is clear that models to predict resistivity and resistance grow more complex, but are not accurate enough to use for practical controllers. These techniques have not yet explained:

- The plastic deformation the actuator incurs over its life.
- Determination of constants for general SMA materials.
- Temperature measurement techniques for very fine wires.
- Temperature prediction techniques where measurement is not possible.
- Change in Poisson's ratio and the elastic modulus during phase transformation.

2.2. Empirical techniques

All of the aforementioned resistance models are difficult to employ for self-sensing since they do not include any model of the hysteresis of the resistance during phase transformation, and require knowledge of parameters that are difficult or impossible to measure (such as the phase fraction and temperature). These concerns are magnified for very thin wire actuators. Attempts have been made to reduce the error of neglecting hysteresis by employing polynomial models to fit the relationship between strain and resistance separately on the heating and cooling paths. However, these models rely on explicit knowledge of the wire stress [5, 6, 25, 26].

One clever solution for elimination of some nonlinear error is to arrange two SMA actuators in antagonistic manner and measure the difference in resistance between them [7, 27]. However, the material behavior is different for antagonist pairs than with single wires, and requires additional consideration during implementation [28]. This method also does not sufficiently eliminate the effects of hysteresis, and cannot account for the effect of differing stress in the two antagonist wires.

Empirical techniques are good for cases where load is known, but not for general actuators. In particular, these techniques still cannot account for:

- The plastic deformation throughout the actuator's lifetime.
- *In situ* fitting to data requires a temporary position sensor.
- Arbitrary changing loads during actuation, or simultaneously changing the loading and temperature conditions of the wire [29].

2.3. Desired self-sensing characteristics

A complete model of shape memory resistivity must capture many aspects of the behavior to provide robust self-sensing. The following are some broad characteristics that a robust self-sensing scheme should include:

- Ability to obtain accurate measurements independent of the wire loading and stresses.
- Ability to obtain accurate measurements for all ambient air temperatures and currents.
- Elimination of any errors associated with the hysteresis stemming from both the shape memory and super-elastic behaviors of SMA actuators.
- Ability to account for wire strains due to fatigue.
- Ability to obtain accurate measurements independent of the specific alloy used.
- Ability to obtain accurate measurements without an exact knowledge of the SMA temperature.

None of the self-sensing models considered to-date can account for all of these important factors. Most existing self-sensing controller schemes employ some form of a simplifying assumption or constraint on the physical model, such as:

- Electrical resistance is linearly proportional to martensite phase fraction [8, 13, 30].

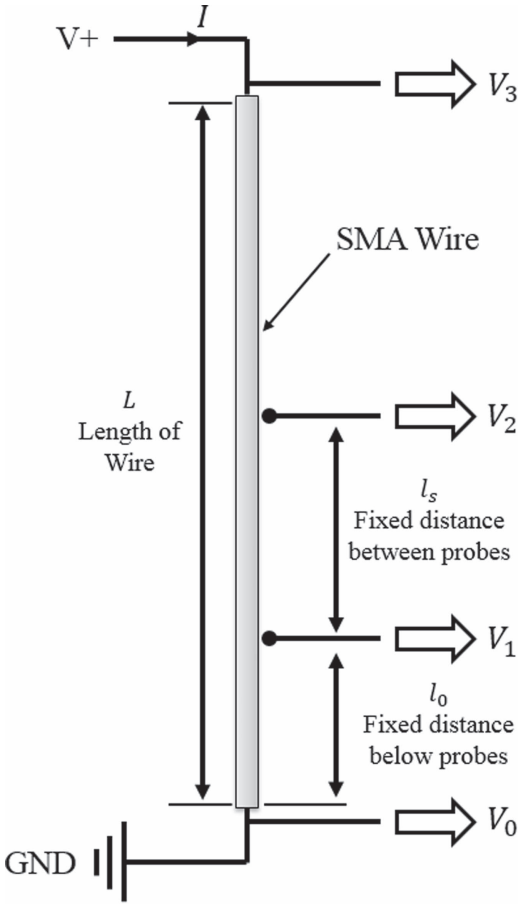

Figure 1. Dual measurement technique schematic.

- Hysteresis between heating and cooling curves is adequately small [10].
- SMA temperature is a known property [15].
- SMA temperature is proportional to input power [6, 22, 23].
- SMA temperature is a constant property [12].
- SMA stress versus actuator length is known or held constant [19, 20, 25].
- For two SMA wires in an antagonist orientation, the wires have the same stress [7, 27].
- Hysteresis is not affected by stress [5].

3. Dual measurement technique

Our measurement system is comprised of two main components. The first is a high-side measurement of voltage across the entire SMA wire (V_3) across and current (I) through the entire SMA wire. The high-side voltage lead is directly connected to the end of the SMA wire, such that it moves as the wire changes length. The second component is a set of two voltage probes (V_1 and V_2), set a fixed distance (l_0) from the stationary end of the wire and a fixed distance from one another (l_s) (figure 1).

The useful quantities that can be computed using the dual measurement are now presented. Because the resistance is considered constant throughout the actuator and the current is constant as well, the voltage drop is linear across the actuator. This yields:

$$\frac{V_3 - V_1}{L - l_0} = \frac{V_2 - V_1}{l_s}. \tag{9}$$

It is then easily shown that, if l_s and l_0 are constant, then:

$$L = l_0 + l_s\left(\frac{V_3 - V_1}{V_2 - V_1}\right). \tag{10}$$

Thus we can directly solve for actuator length with no knowledge of the actuator properties besides initial length and slider position, nor a model of the material. This is only accurate if the material properties are equal along the entire length of the wire, thus it provides a better estimate for larger l_s. Because sensor noise is unavoidable, it is best to maximize the denominator in equation (9) by having l_s as large as is practical, and l_0 as small as is practical. Thus, if possible, V_1 should be measured at ground ($l_0 = 0$), and l_s should be as close to the contracted length of the wire as possible. This also reduces inaccuracies arising due to varying conditions along the length of the wire because only three portions of the wire need to be electrically connected instead of four. If these recommendations are heeded, then the model reduces to

$$L = l_s\left(\frac{V_3}{V_2}\right). \tag{11}$$

Notice that this provides the total length without ever measuring the total length. This alone could be beneficial in manufacturing where the lengths may not be consistent. The electrical resistivity is easily calculated using:

$$\rho = \left(\frac{A}{l_s}\right)\frac{(V_2 - V_1)}{I}. \tag{12}$$

Table 1. Example SMA actuator characteristics.

Characteristic	Value
Initial (hot) length	160 mm
Cold length	168.1 mm
Diameter	0.125 mm
Mass	12.6 mg
Expected A_f	90 °C
Treatment	Kroll's reagent
Manufacturer	Dynalloy Flexinol HT

4. Experimental setup

The device being tested is a simple, straight SMA wire. The physical characteristics of the wire are listed in table 1, where A_f is the austenite finish temperature at which the wire is nominally fully contracted, according to the manufacturer [31].

The experiment is performed on a custom-built dynamic tensile testing machine that implements the features of

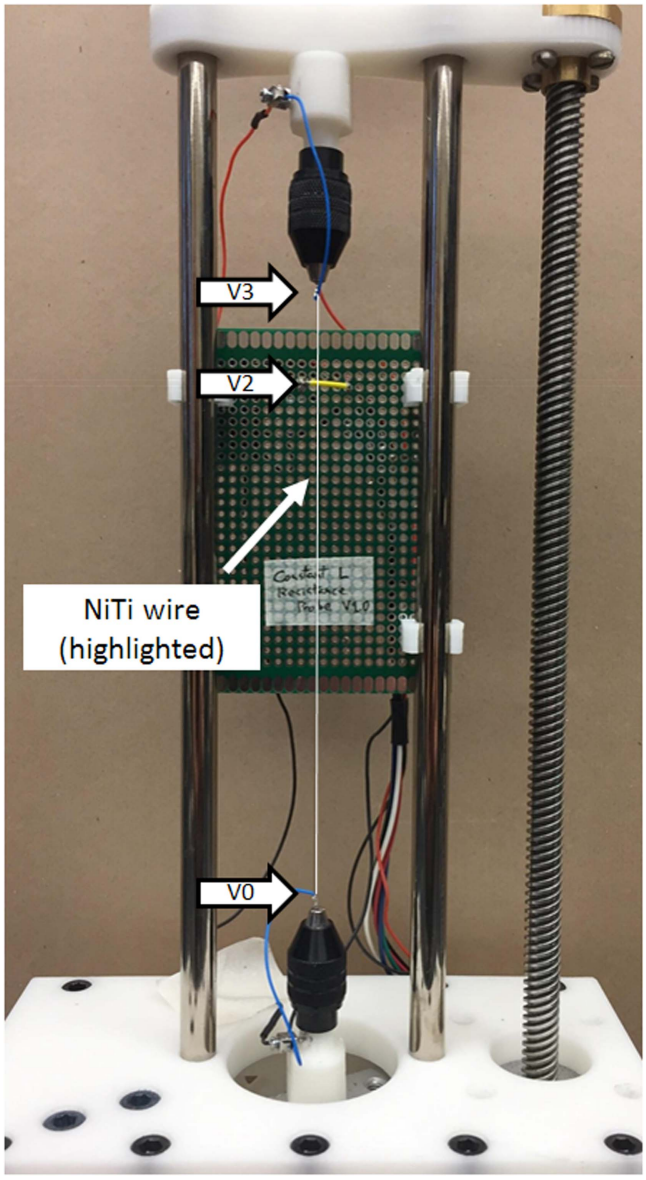

Figure 2. Tensile testing machine.

figure 1 (figure 2). This machine controls the electrical input to the SMA actuator, and simulates a system for the SMA actuator to control. In this experiment, the simulated system is a simple suspended mass subjected to a constant force.

The V_3 voltage lead is soldered to the end of the SMA wire, such that it moves as the wire changes length. Two voltage probes (V_0 and V_2) make sliding contact with the SMA wire on a 1.5 mm Chrome-plated steel cylinder (figure 3). Note that this configuration corresponds with $l_0 = 0$.

These probes are mounted on a plate in the testing machine such that they can be moved up and down to change l_s.

Electric current is controlled through the SMA wire in a slow saw-tooth manner, and the load is regulated. Three simulated masses are used; 100 grams (gm), 200 gm, and 300 gm. By repeating the test with these different loads, we will see that the model can estimate actuator length regardless

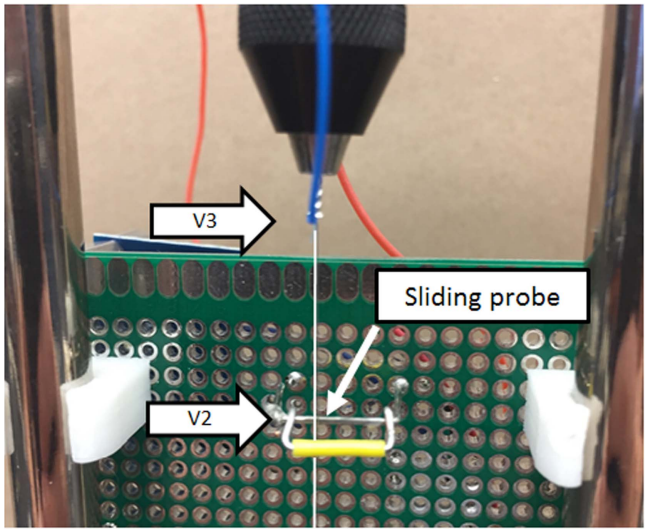

Figure 3. Sliding probe for second measurement. Note that the yellow bar prevents wire tangling while slack.

of the stress applied—a valuable result for robust sensing. The ambient temperature is approximately 25 °C throughout the duration of the test.

5. Characterization experiment

The experimental results validate the dual measurement technique. The experiment is performed in 3 parts. The driving input is SMA current, driven from 40 to 250 mA in a saw-tooth manner, and the load is regulated to 300, 200 and 100 gram-force during three current sweeps (figure 4).

The stresses due to these loads are approximately 80, 160, and 240 MPa, respectively. The ambient temperature is approximately 25 °C throughout the duration of the test, though no enclosure is provided to limit air currents since that is not typically realistic for general actuators. Before each new load, the actuator is allowed to stabilize at the new equilibrium position—measurements during this transition are not recorded (causing data discontinuity at 40 and 80 s). The initial position, with the wire completely heated with no load is listed in table 2.

6. Characterization test results

The test shows the inadequacy of assuming the resistance directly relates to actuator strain; electrical resistance is plotted against true actuator displacement in figure 5. Also, a line is fit through the data using least squares, and percent error is calculated from the difference between resistance and this line.

Several observations can be made about this plot:

- The main trend of resistance versus actuator displacement is linear away from the transformation boundaries.
- There is large hysteresis when near 100% martensite (longest length).

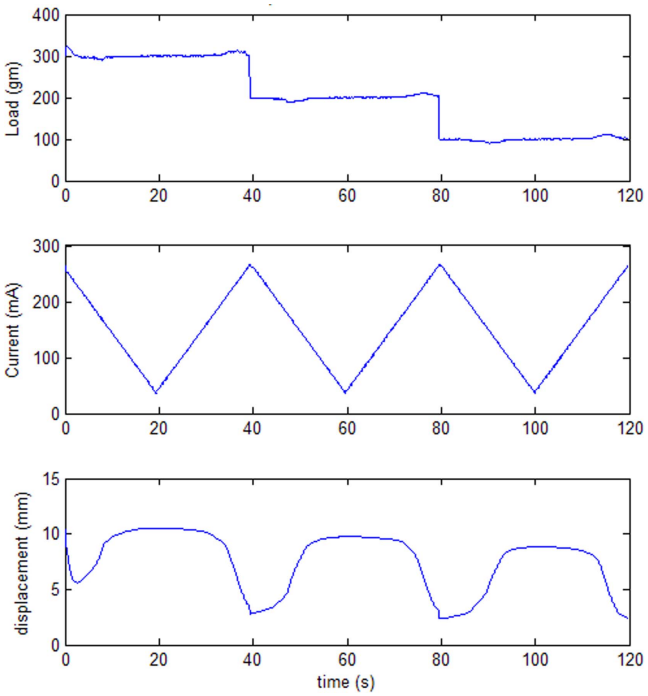

Figure 4. Driving inputs for the experiment are three loads held constant (top) while current is swept in a saw-tooth manner (middle) which extends and contracts the actuator (bottom).

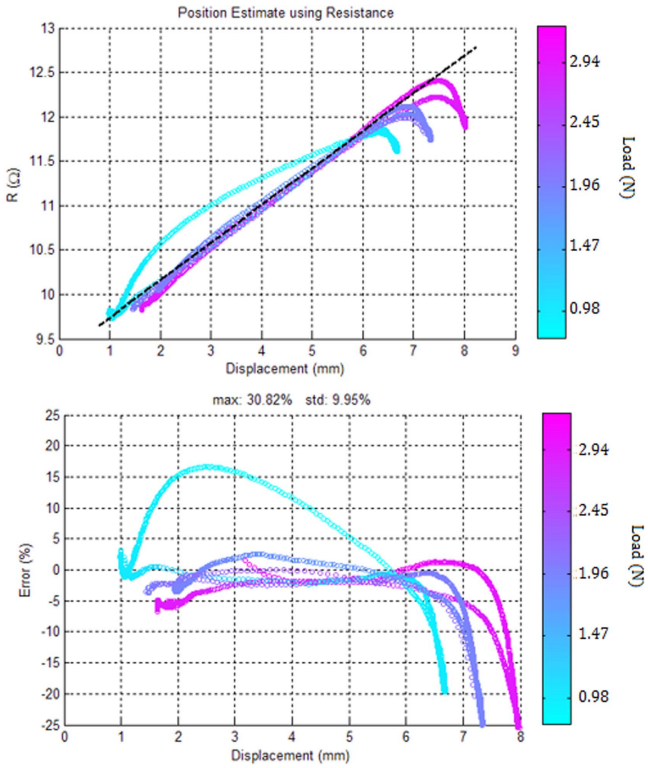

Figure 5. Self-sensing displacement measurements and errors using SMA resistance versus actual displacement (colored by loading condition). Resistance of the SMA wire, by itself, makes a poor displacement sensor due to combined effects of elastic strain, temperature, and shape memory hysteresis.

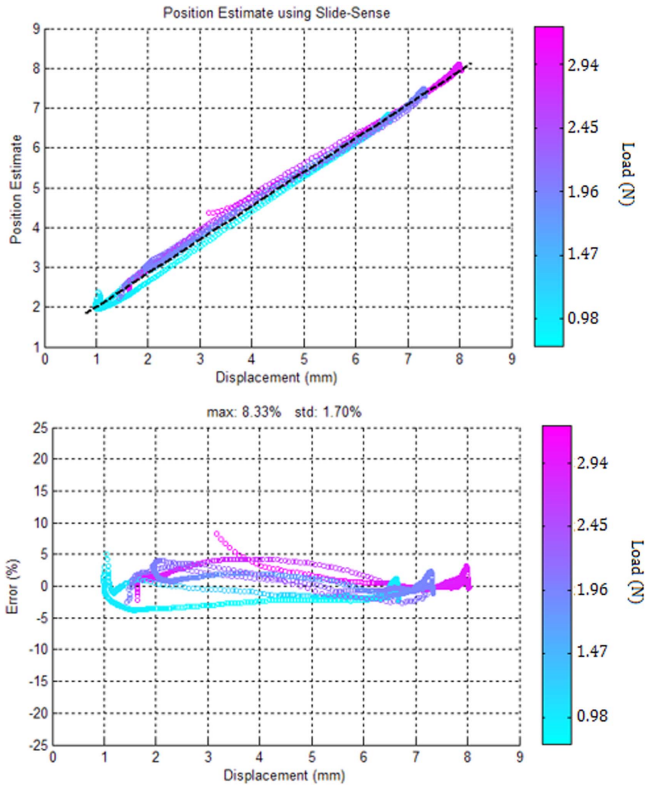

Figure 6. Self-sensing displacement measurement and errors using dual voltage measurement technique (colored by loading condition).

Table 2. SMA actuator parameters required for length calculation.

Distance	Value
L	160 mm
l_s	55 mm
l_0	91 mm

- There is a very wide hysteresis band at low load (100 gf or 0.98 N).
- The relationship between resistance and displacement reverses near the ends due to temperature effects.

By computing a length estimate using equation (9), we can directly calculate the actuator length as seen in figure 6. The estimate is very linear and matches well to the measured position.

The estimate becomes accurate soon after the wire touches the probe—this can be seen in the middle of the plot as the wire initially heats and contacts the sliding probe (near 3 mm).

7. Feedback control experiments

An experiment was performed to determine the ability of the sliding-sensing method, compared to feedback with a position encoder, and feedback using the assumption that length is linearly related to wire length. The linear fits used are shown in figures 5 and 6 as dashed black lines.

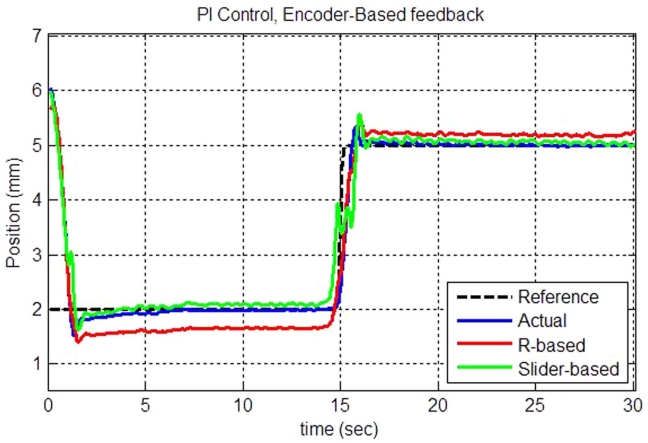

Figure 7. Wire position feedback with 200 gf load (1.96 N).

The dynamic tensile testing machine was used to provide a constant antagonist force while the SMA wire was controlled using a PI feedback controller with a regulated current input. The controller is Type 1, and as such has zero steady state error with an unbiased measurement of position. The bandwidth of the machine is much higher than the bandwidth of the SMA actuator, which is characteristically very low [32–35], and so its dynamics do not directly affect the SMA controller. The control experiment maintains a constant load on the SMA wire while a position set-point is changed. The load is regulated to 100, 200 and 300 gf (0.98 N, 1.96 N, and 2.94 N, respectively) during each experiment, respectively, to determine whether the two self-sensing techniques are reliable with changing loads. The experiment using the encoder serves as a reference to ensure the controller is capable of tracking the reference, and so any error is due to flaws in the self-sensing method.

8. Controller test results

The three trials showed nearly consistent results, with the encoder providing better accuracy. The dual measurement self-sensing technique provides nearly as accurate a measurement as the encoder, while the resistance based position measurement lacks the accuracy of the encoder or the dual measurement technique's measurements. The control reference was set to two different points, ensuring the sensing method was accurate across the range of SMA wire motion. To understand the control motion and the meaning of positioning accuracy, the performance of the control using encoder feedback is provided (figure 7).

The controller quickly drives the system to the desired set-points, settling in less than five seconds at each point. By observing the resistance and slide-sense position estimates during this test, we get a first understanding of the inaccuracy they will induce. The resistance-based method has large deviations from the true position both dynamically and in steady-state. The slider-based self-sensing is accurate and nearly matches the encoder position measurement.

A better presentation of the relative accuracies of these three methods is given by using the respective position estimates for controller feedback. By comparing the tracking error between different methods (encoder, resistance, and slide-sense feedback), and loadings (100, 200, and 300 gf loads or 0.98, 1.96, and 29 N loads), the full operating range can be seen (figure 8).

First looking to the encoder feedback, we see the performance of the PI controller. In all cases, the controller is able to regulate the position with no steady-state error. The controller stabilizes the system within five seconds in all cases. At high loads, the controller has some difficulty stabilizing at the second set-point when the wire is soft (cold, long) after fifteen seconds in each test. This is due to the decrease in the plant natural frequency (lower spring rate, increased load), which has shifted the problem such that the controller gain is too high for the plant. This is not a problem in this experiment, but it shows the value of reviewing encoder feedback to know this is an effect of the controller, not the sensing method. Furthermore, this issue could be resolved through the use of more advanced control techniques such as adaptive control laws to completely mitigate the issue.

The resistance-based feedback shows two primary flaws. First, the initial accuracy in the measurement is very poor, as this is when the wire is completely cold and in either a twinned martensite or *R*-phase state, so the hysteresis error is exaggerated. Because of the simple PI control law, this causes a 'windup' in the integrator, and impacts the stability of the system (slowing down tracking and causing nonlinear overshoot). At high loads, the windup of the integrator is particularly poor. While this can partially be avoided by incorporating anti-integrator windup feedback, a more accurate measurement technique could allow for an avoidance of this complication altogether. The second primary concern of this measurement technique is that the hysteresis in the heating and cooling response for the electrical resistance causes steady-state error in the regulator—the system is never driven to the correct position because the resistance measurement has error that is never resolved.

The dual-measurement feedback quickly provides an accurate estimate of the position. The controller has no steady state error because the method provides a linear, unbiased estimate, except in the case of a very high load. At such a high load, the controller scheme does have some steady state error because the physical sliding probes deflected slightly under the pressure of the taut wire and this physical movement altered the measurement. For a more robust conductive probe, this concern is eliminated. The dual measurement technique does fall short of the encoder with respect to the signal noise, as the sliding does generate some electrical noise, and the resolution of the voltage measurements is a limiting factor.

9. Conclusions and discussion

In more than thirty repeated tests, the measurement error is typically banded within 0.5 mm of the true length. This is true even as the wire shows permanent deformation in the form of

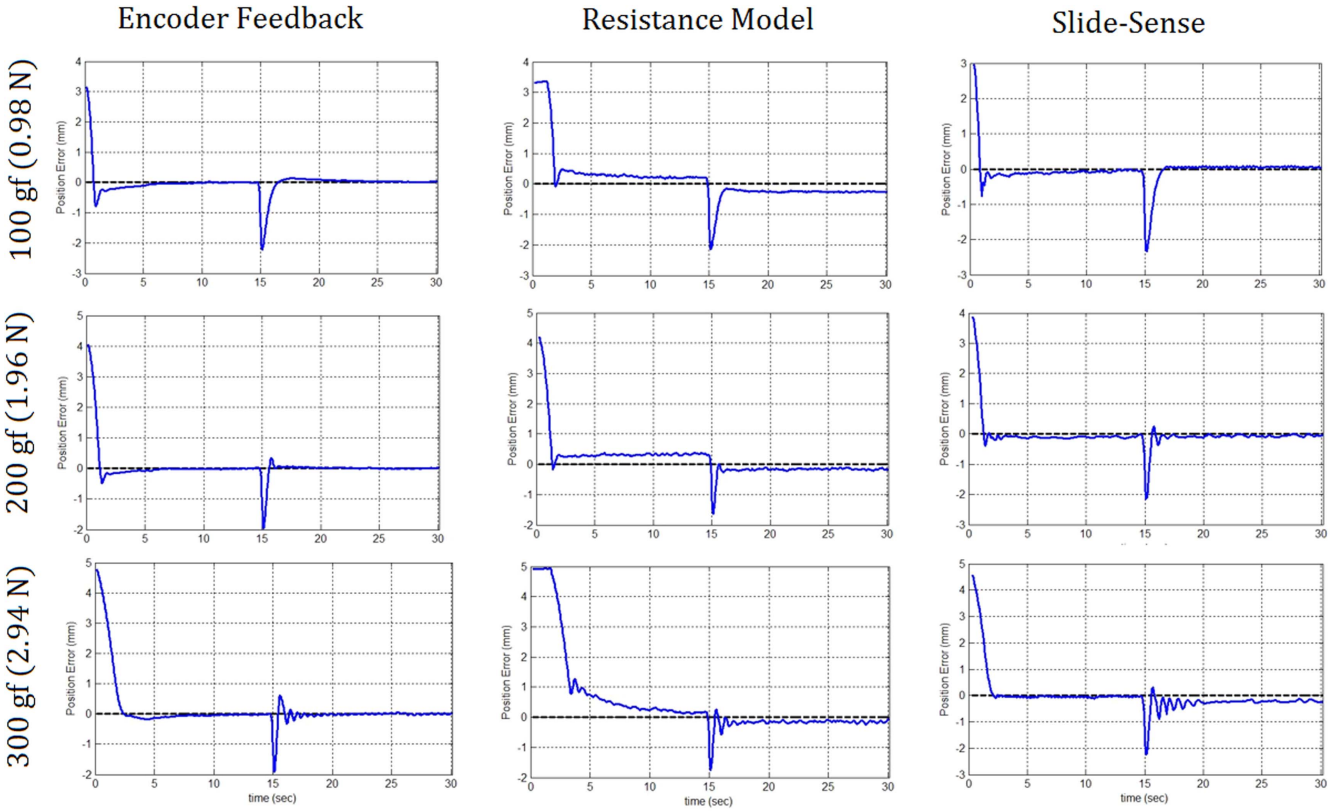

Figure 8. Position error using encoder feedback, resistance model of self-sensing, and the slide-sense technique at three antagonist loads.

fatigue with repeated cycling. Error is calculated by subtracting the estimated length from the true length; the error in all experiments shows standard deviation of error of 0.154 mm. As an actuator, we often care about the error as a percentage of the total travel, not length. With an effective stroke of 8.2 mm in the 160 mm wires used, this implies 1.7% standard deviation. For comparison, the linear resistance assumption provides a 9.95% standard deviation of error. Noise in the estimate appears to be solely related to noise in the voltage measurements made. Hardware or software filtering can effectively improve the noise.

In a control scenario using a generic, stabilizing PI control law, the slide-sense method provides an unbiased, accurate estimate of position. The method is consistent until the test setup was physically bent due to high load on the probe. For comparison, the resistance feedback method shows integrator windup errors and steady-state error, both due to real hysteresis in the wire.

The dual measurement technique has allowed us to estimate the length of a general SMA wire without prior knowledge of:

- Macroscopic electro-mechanical material properties of the SMA actuator.
- Applied loads and temperature conditions of the wire.
- Ambient conditions of the cooling fluid.
- The electric current being passed through the SMA actuator.
- The initial wire geometry or configuration.

Thus we have created a robust mechanism for self-sensing in SMA actuators for use in robotics applications. Without a sensor for feedback, accurate robots cannot be built; the dual measurement technique has the potential to make SMA actuators more cost effective by eliminating the need for position sensors. It also allows the actuators to be smaller and to fit more DoF in a smaller space. Dual measurement provides a reliable and simple technique to implement robust self-sensing in SMA actuators.

The dual measurement method eliminates the major sources of error in existing methods, but introduces some new concerns:

- The wire surface must be conductive, meaning to use this method a surface treatment will be required.
- Corrosion of probe contact surface may affect the quality of the measurement over time.
- Sliding contact may decrease the life of the SMA actuator.
- Electrical noise in the form of Nyquist–Johnson noise or inaccuracies due to discretization in the ADC.
- End crimps or solder affects measurement accuracy for short wires.
- The assumption of constant resistance across the wire may not hold for short wires due to the effects of boundary conditions (this concern is alleviated for wires over 14.8 cm in length) [36].

Future work will study these potential issues. Superior surface finish of the wire could prove to eliminate corrosion

and maintain electrical conductivity. Improved mechanical design of the sliding contact can eliminate wear—techniques from electric motors and slip rings may be adopted for this purpose. Electrical noise is directly related to the quality of the ADC and the level of filtering used. Empirical evidence suggestions that placement of the sliding probe affects the amount of electrical noise. In situations where the sample rate is fast compared to the required sensing bandwidth, software or hardware filtering can significantly eliminate the noise.

Acknowledgments

This work was supported by the Alabama Space Grant Consortium, NASA Training Grant NNX15AJ18H.

ORCID iDs

Tyler Ross Lambert https://orcid.org/0000-0002-8802-9232

References

[1] Schaal S, Atkeson C and Vijayakumar S 2000 Real-time robot learning with locally weighted statistical learning *Int. Conf. on Robotics & Automation (San Francisco, CA)*
[2] Moeslund T B, Hilton A and Krüger V 2006 A survey of advances in vision-based human motion capture and analysis *Comput. Vis. Image Underst.* **104** 90–126
[3] Ma R R and Dollar A M 2011 On dexterity and dexterous manipulation *Int. Conf. on Advanced Robotics (Tallinn, Estonia)*
[4] Lewinger W A, Branicky M S and Quinn R D 2006 Insect-inspired, actively compliant hexapod capable of object manipulation *Climbing and Walking Robots* (Berlin: Springer) (https://doi.org/10.1007/3-540-26415-9_7)
[5] Lan C-C and Fan C-H 2010 An accurate self-sensing method for the control of shape memory alloy actuated flexures *Sensors Actutators* A **163** 323–32
[6] Wang T-M, Shi Z-Y, Liu D, Ma C and Zhang Z-H 2012 An accurately controlled antagonist shape memory alloy actuator with self sensing *Sensors* **12** 7682–700
[7] Josephine R, Sunjai N and Dhanalakshmi K 2014 Differential resistance feedback control of a self-sensing shape memory alloy actuated system *Int. Soc. Autom. Trans.* **53** 289–97
[8] Yang K and Gu C L 2002 A novel robot hand with embedded shape memory alloy actuators *Proc. Inst. Mech. Eng.* C **216** 737–45
[9] Simone F, York A and Seelecke S 2015 Design and fabrication of a three-finger prosthetic hand using SMA muscle wires *Proc. SPIE* **9429** 94290T
[10] Pozzi M and Airoldi G 1999 The electrical transport properties of shape memory alloys *Mater. Sci. Eng.* A **A273** 300–4
[11] He Z, Gall K and Brinson L 2006 Use of electrical resistance testing to redefine the transformation kinetics and phase diagram for shape memory alloys *Metall. Mater. Trans.* A **37A** 579–87
[12] Wu X D, Wu J S and Wang Z 1999 The variation of electrical resistance of near stoichiometric NiTi during thermo-mechanic procedures *Smart Mater. Struct.* **8** 574–8
[13] Ikuta K, Tsukamoto M and Hirose S 1988 Shape memory alloy servo actuator system with electric resistance feedback and application for active endoscope *Proc. 1988 Int. Conf. on Robotics and Automation (Philadelphia)* (https://doi.org/10.1109/ROBOT.1988.12085)
[14] Ikuta K, Tsukamoto M and Hirose S 1991 Mathematical model and experimental verification of shape memory alloy for designing micro actuator *Micro Electro Mechanical Systems (MEMS '91) Proc. An investigation of Micro Structures, Sensors, Actuators, Machines, and Robots IEEE (Nara)*
[15] Antonucci V, Faiella G, Giordano M, Mennella F and Nicolais L 2007 Electrical resistivity study and characterization during NiTi phase transformation *Thermochimica Acta* **462** 64–9
[16] Uchil J, Ganesh Kumara K and Mahesh K 2002 Effect of thermal cycling on R-phase stability in a NiTi shape memory alloy *Mater. Sci. Eng.* A **332** 25–8
[17] Novak V, Sittner P, Dayananda G, Braz-Fernandes B and Mahesh K 2008 Electrical resistance variation of NiTi shape memory alloy wires in thermomechanical tests: experiments and simulation *Mater. Sci. Eng.* A **481–482** 127–33
[18] Song H, Kubica E and Gorbet R 2011 Resistance modelling of SMA wire actuators *Int. Workshop at the Smart Materials, Structures & NDT in Aerospace (Montreal)*
[19] Zhang J and Yin Y 2012 SMA-based bionic integration design of self-sensor-actuator-structure for artificial skeletal muscle *Sensors Actuators* A **181** 94–102
[20] Zhang J-J, Yin Y-H and Zhu J-Y 2013 Electrical resistivity-based study of self-sensing properties for shape memory alloy-actuated artificial muscle *Sensors* **13** 12958–74
[21] Cui D, Song G and Li H 2010 Modeling of the electrical resistance of shape memory alloy wires *Smart Mater. Struct.* **19** 1–8
[22] Lewis N, York A and Seelecke S 2013 Experimental charcterization of self-sensing SMA actuators under controlled convective cooling *Smart Mater. Struct.* **22** 1–10
[23] Furst S and Seelecke S 2012 Modeling and experimental characterization of the stress, strain, and resistance of shape memory alloy actuator wire with controlled power input *J. Intell. Mater. Syst. Struct.* **23** 1233–47
[24] Furst S, Crews J and Seelecke S 2013 Stress, strain, and resistance behavior of two opposing shape memory alloy actuator wires for resitsancebased self-sensing applications *Intell. Mater. Syst. Struct.* **24** 1951–68
[25] Lan C-C, Lin C-M and Fan C-H 2011 A self-sensing microgripper module with wide handling ranges *IEEE/ASME Trans. Mechatronics* **16** 141–50
[26] Liu S-H, Huang T-S and Yen J-Y 2010 Tracking control of shape-memory-alloy actuators based on self-sensing feedback and inverse hysteresis compensation *Sensors* **10** 112–27
[27] Josephine Sevarani Ruth D, Dhanalakshmi K and Sunjai Nakshatharan S 2015 Bidirectional angular control of an integrated sensor/actuator shape memory alloy based system *Measurement* **69** 210–21
[28] Georges T, Brailovski V and Terriault P 2012 Characterization and design of antagonistic shape memory alloy actuators *Smart Mater. Struct.* **21** 1–8
[29] Elahinia M and Ahmadian M 2005 An enhanced SMA phenomenological model: I. The shortcomings of the existing models *Smart Mater. Struct.* **14** 1297–308
[30] Ikuta K, Tsukamoto M and Hirose S 1991 Mathematical model and experimental verification of shape memory alloy for designing micro actuator *Micro Electro Mechanical Systems (Nara)* (https://doi.org/10.1109/MEMSYS.1991.114778)
[31] Dynalloy Inc., 'Technical Characteristics of Flexinol Actuator Wires,' Irvine, CAhttp://www.dynalloy.com/pdfs/TCF1140.pdf
[32] Lambert T R, Gurley A and Beale D 2016 Heat transfer modelling and bandwidth determination of SMA acuators in

robotics applications *Early Career Technical Conf. (Birmingham)*
[33] Ditman J, Bergman L and Tsao T-C 1996 The design of extended bandwidth shape memory alloy actuators *J. Intell. Mater. Syst. Struct.* **7** 635–45
[34] Nakshatharan S, Kaliaperumal D and Ruth D 2016 Effect of stress on bandwidth of antagonistic shape memory alloy actuators *J. Intell. Mater. Syst. Struct.* **7** 153–65
[35] Song G *et al* 2003 A neural network inverse model for a shape memory alloy wire actuator *J. Intell. Mater. Syst. Struct.* **14** 371–7
[36] Furst S J *et al* 2012 Numerical and experimental analysis of inhomogeneities in SMA wires induced by thermal boundary conditions *Contin. Mech. Thermodyn.* **10** 497